# Sensitivity Analysis for Nonlinear Heat Conduction

**Kevin J. Dowding**
e-mail: kjdowdi@sandia.gov

**Bennie F. Blackwell**
e-mail: bfblack@sandia.gov

Sandia National Laboratories,
P.O. box 5800, Mail Stop 0828,
Albuquerque, NM 87185-0828

*Parameters in the heat conduction equation are frequently modeled as temperature dependent. Thermal conductivity, volumetric heat capacity, convection coefficients, emissivity, and volumetric source terms are parameters that may depend on temperature. Many applications, such as parameter estimation, optimal experimental design, optimization, and uncertainty analysis, require sensitivity to the parameters describing temperature-dependent properties. A general procedure to compute the sensitivity of the temperature field to model parameters for nonlinear heat conduction is studied. Parameters are modeled as arbitrary functions of temperature. Sensitivity equations are implemented in an unstructured grid, element-based numerical solver. The objectives of this study are to describe the methodology to derive sensitivity equations for the temperature-dependent parameters and present demonstration calculations. In addition to a verification problem, the design of an experiment to estimate temperature variable thermal properties is discussed.* [DOI: 10.1115/1.1332780]

*Keywords:* *Conduction, Parameter Estimation, Heat Transfer*

## Introduction

Temperature dependence of parameters in the heat conduction equation must be accounted for in many problems. For example, thermal conductivity, volumetric heat capacity, convection coefficients, emissivity, contact conductance, and source terms may demonstrate a dependence on temperature. Except for relatively simple situations where closed form analytical solution can be derived, obtaining a solution when parameters depend on temperature requires a numerical method. A common numerical method is to approximate the temperature dependence via basis functions, such as piecewise-linear. Parameters in the functions that describe the temperature dependence may be known with varied levels of accuracy. In many instances, data are only available at discrete temperatures and the analyst must use engineering judgment to approximate the behavior between data points. Knowing the sensitivity of the solution to parameters that describe the temperature dependence would be valuable to the thermal analyst. Sensitivity analysis for nonlinear heat conduction owing to temperature-dependent properties is the focus of this paper.

Sensitivity analysis determines the partial derivative of the state variable (temperature for thermal problems) with respect to model parameters (thermal conductivity, volumetric heat capacity, convection coefficient, emissivity, etc.). This partial derivative is called a sensitivity coefficient. Although valuable insight may be gleaned from sensitivity coefficients in their own regard, there are many other applications as well. They are used in parameter estimation ([1–3]); optimal experimental design ([4–7]); and uncertainty or error analysis ([8–10]).

Previous formulations for sensitivity analysis are closely related to perturbation based methods. Probabilistic finite elements of structural dynamics are studied for linear ([11]) and nonlinear ([12]) cases. Emergy and Fadale [13] present a formulation for nonlinear heat conduction, which extends their prior work for the linear problem ([10]). Thermal properties are treated as random field parameters in Nicolai and De Baerdermaeker [14,15].

There are several approaches to calculate sensitivities ([16]). The method used here is to differentiate the describing equations with respect to parameters to derive sensitivity equations that are numerically solved. All previously cited references use a similar approach, with one difference. In this paper continuum equations, instead of discrete equations, are used to derive the sensitivity equations. Previous investigations ([11–15]) have derived the sensitivity equations from discrete describing equations. While the two approaches may result in the same numerical value for sensitivity, we believe there is additional insight available from the sensitivity equations as derived in this paper, which is not available from previous approaches.

Temperature dependence of parameters is discussed next. Sensitivity equations for nonlinear heat conduction are derived and discussed in the following section. Then numerical examples are shown including a verification problem and model of an experiment being designed to estimate temperature-dependent thermal properties of a low thermal conductivity material (polyurethane foam).

## Temperature-Dependent Parameters

Temperature dependence of parameters can be represented in various ways. For generality, temperature dependence of parameter $g(T)$ is assumed to have an arbitrary functional form

$$g(T)=\sum_{j=1}^{N_g} g_j\theta_j^g(T). \tag{1}$$

Eq. (1) could, for example, be piecewise linear or a spline function, where $g_j$ are constants, and $\theta_j^g(T)$ is the $j^{\text{th}}$ basis function describing parameter $g(T)$; there are $N_g$ terms to describe $g(T)$. It is possible that different temperature-dependent parameters will use different approximations. Representing the temperature dependence, as shown in Eq. (1), allows for generality and flexibility. Furthermore, temperature-dependent functions are parametrized—i.e., represented with a series of constant parameters. Consequently, standard calculus can be used to compute sensitivity (derivatives). Another approach is to consider the temperature-dependent parameters as functions, i.e., infinite-dimensional. In this case variational methods are needed to calculate the derivatives. This approach is not considered further in this paper but may be a more efficient way to get sensitivity to temperature-dependent functions.

Using Eq. (1) temperature-dependent parameters are represented as a collection of constant parameters. The number of parameters that represent the temperature dependence (and associated basis functions) can vary by parameter. We have solved problems that require nominally 5–10 parameters to describe the temperature dependence of a thermal property and/or boundary

Contributed by the Heat Transfer Division for publication in the JOURNAL OF HEAT TRANSFER. Manuscript received by the Heat Transfer Division October 5, 1999; revision received August 23, 2000. Associate Editor: S. Sadhal.

  

coefficient. Hence when multiple materials with temperature-dependent properties are present, the total number of parameters can become quite large; hundreds of sensitivity coefficients may be required. In this study only first-order sensitivity is discussed. Computational requirements for second-order analysis are significantly greater ([16]).

Sensitivity analysis, as will be shown later, requires the derivative of the function $g(T)$ with respect to temperature. The derivative can be related to the original description as

$$\frac{dg(T)}{dT}=\sum_{j=1}^{N_g} g_j \phi_j^g(T), \tag{2}$$

where

$$\phi_j^g(T)\equiv\frac{d\theta_j^g(T)}{dT}. \tag{3}$$

The derivative $dg(T)/dT$ in Eq. (2) will have the same coefficients, $g_j$, as the function $g(T)$ in Eq. (1). Basis functions for $dg(T)/dT$, however, are the derivative (with respect to temperature) of the basis functions for $g(T)$; see Eq. (3). We note that it is possible that the derivative of the basis function will be discontinuous. An example is a piecewise linear function, which would have a discontinuous derivative at points joining linear segments with different slopes.

## Equation for Nonlinear Heat Conduction

Sensitivity equations for general nonlinear heat conduction are derived in this section. Equations are implemented in an unstructured grid, control-volume finite-element code. Hence, an integral equation description is presented. An analogy to the differential formulation of the equations is straightforward ([17]). Sensitivity equations in this paper extend the work in ([16]), which considered linear heat conduction with constant parameters. Prior to discussing sensitivity equations, a formulation for the temperature field is presented.

**Temperature Equations.** The integral energy equation for a multidimensional body with temperature-dependent thermal properties and source term is

$$\int\int_V\int C(T)\frac{\partial T}{\partial t}d\mathcal{V}+\int_{\mathcal{A}}\int \vec{q}\cdot d\vec{\mathcal{A}}=\int\int_{\mathcal{V}}\int \dot{e}'''(T)d\mathcal{V}. \tag{4}$$

The heat flux is represented with Fourier's Law

$$\vec{q}=-\tilde{\mathbf{k}}(T)\cdot\nabla T, \tag{5}$$

where $\tilde{\mathbf{k}}(T)$ can be, in general, a full thermal conductivity tensor. In this work $\tilde{\mathbf{k}}(T)$ only has diagonal entries that represent an orthotropic material

$$\tilde{\mathbf{k}}(T)=\begin{bmatrix} k_{11}(T) & 0 & 0 \\ 0 & k_{22}(T) & 0 \\ 0 & 0 & k_{33}(T)\end{bmatrix}. \tag{6}$$

Flux conditions are prescribed on part of the boundary ($\mathcal{A}_b$) with the three types of prescribed heat flux (constant, convection, and radiation) written in a single equation of the form

$$\int_{\mathcal{A}_b}\int \vec{q}\cdot d\vec{\mathcal{A}}=\int_{\mathcal{A}_b}\int -(\tilde{\mathbf{k}}(T)\cdot\nabla T)_{\vec{x}_b}\cdot d\vec{\mathcal{A}}=\int_{\mathcal{A}_b}\int \dot{q}_b''\hat{n}\cdot d\vec{\mathcal{A}}, \tag{7}$$

where

$$\dot{q}_b''=\begin{cases} \dot{q}_0'' & \text{along } \vec{x}_{b_1} \\ \dot{q}_c''=h(T)(T-T_\infty) & \text{along } \vec{x}_{b_2}. \\ \dot{q}_r''=\varepsilon(T)\sigma(T^4-T_r^4) & \text{along } \vec{x}_{b_3}\end{cases} \tag{8}$$

Convection coefficient and emissivity are assumed to be temperature-dependent. A temperature condition is prescribed along the remaining boundary

$$T(\vec{x}_{b_4})=T_b. \tag{9}$$

The initial condition is

$$T|_{t=0}=T_0. \tag{10}$$

**Sensitivity Equations**

*Definition.* Although there are other dependent variables for which sensitivity is important, sensitivity coefficients related to temperature are studied in this paper. The sensitivity coefficient is the partial derivative of temperature with respect to a parameter, which is $\partial T/\partial p_i$ for a parameter $p_i$. Scaling allows sensitivity coefficients for different parameters to be directly compared. A scaled sensitivity coefficient is

$$T_{p_i}\equiv p_i\frac{\partial T}{\partial p_i}. \tag{11}$$

Scaled sensitivity coefficients have units of temperature, allowing magnitudes for different parameters to be directly compared to temperature scales — e.g., magnitude of the transient temperature rise—within the problem.

*Describing equations.* To derive scaled sensitivity equations, the energy equation in Eq. (4) is differentiated with respect to an arbitrary parameter, $p_i$, which represents the $i^{\text{th}}$ parameter describing $p(T)$, and multiplied by that parameter. (While sensitivity is being computed for parameter $p(T)$, the equations have other temperature-dependent parameters, which are arbitrarily referred to in the coming discussion as $g(T)$. Only one parameter satisfies $p(T)=g(T)$). Note that the parameter $p_i$ is assumed to be independent of time and space so that it can be moved inside the integral sign. Differentiating Eq. (4), multiplying by the parameter, and interchanging the order of differentiation and integration results in

$$\int\int_{\mathcal{V}}\int p_i\frac{\partial C(T)}{\partial p_i}\frac{\partial T}{\partial t}d\mathcal{V}+\int\int_{\mathcal{V}}\int C(T)\frac{\partial T_{p_i}}{\partial t}d\mathcal{V}$$
$$+\int_{\mathcal{A}}\int\left(p_i\frac{\partial\vec{q}}{\partial p_i}\right)\cdot d\vec{\mathcal{A}}=\int\int_{\mathcal{V}}\int p_i\frac{\partial\dot{e}'''(T)}{\partial p_i}d\mathcal{V}. \tag{12}$$

The dependent variable in Eq. (12) is $T_{p_i}$. The partial derivative with respect to the heat flux is addressed first. Expanding the third term of Eq. (12), after substituting from Fourier's law, gives

$$p_i\frac{\partial\vec{q}}{\partial p_i}=p_i\frac{\partial}{\partial p_i}[-\tilde{\mathbf{k}}(T)\cdot\nabla T]=-\tilde{\mathbf{k}}(T)\cdot\nabla T_{p_i}-p_i\frac{\partial\tilde{\mathbf{k}}(T)}{\partial p_i}\cdot\nabla T. \tag{13}$$

The differentiation process results in partial derivatives of temperature-dependent parameters—for example $p_i\partial\tilde{\mathbf{k}}(T)/\partial p_i$ in Eq. (13). First, we write these partial derivatives for an arbitrary parameter, $g(T)$. By taking the partial derivative of Eq. (1), the derivative of an arbitrary temperature-dependent parameter is obtained

$$p_i \frac{\partial g(T)}{\partial p_i} = \sum_{j=1}^{N_g} g_j p_i \frac{\partial \theta_j^g(T)}{\partial p_i} + \begin{Bmatrix} g_i \theta_i^g(T) & p=g \\ 0 & \text{otherwise} \end{Bmatrix}. \quad (14)$$

Using the chain rule, the first term on the right side of Eq. (14) can be related to the derivative of $g(T)$

$$\sum_{j=1}^{N_g} g_j p_i \frac{\partial \theta_j^g(T)}{\partial p_i} = \sum_{j=1}^{N_g} g_j \frac{d\theta_j^g(T)}{dT} p_i \frac{\partial T}{\partial p_i} = \frac{dg(T)}{dT} T_{p_i}. \quad (15)$$

The final expression in Eq. (15) follows from the derivative defined in Eqs. (2) and (3). Equation (14) can be rewritten with the result of Eq. (15) as

$$p_i \frac{\partial g(T)}{\partial p_i} = \frac{d_g(T)}{dT} T_{p_i} + \begin{Bmatrix} g_i \theta_i^g(T) & p=g \\ 0 & \text{otherwise} \end{Bmatrix}. \quad (16)$$

The partial derivative of a temperature-dependent parameter has two contributions. The first term on the right side of Eq. (16) arises for all temperature-dependent parameters, regardless of $p_i$. It is the derivative of the parameter, with respect to temperature, multiplied by the scaled sensitivity coefficient. The second term in Eq. (16) is only nonzero when the parameter $p_i$ is a coefficient describing the function—i.e., $p=g$.

The derivative of the thermal conductivity tensor, with respect to the parameter $p_i$ in Eq. (13), can be written as

$$p_i \frac{\partial \tilde{\mathbf{k}}(T)}{\partial p_i} = \frac{d\tilde{\mathbf{k}}(T)}{dT} T_{p_i} + \begin{Bmatrix} k_{ll,i} \theta_i^{k_{ll}}(T) & p=k_{ll} \\ 0 & \text{otherwise} \end{Bmatrix}. \quad (17)$$

The final term on the right side of Eq. (17) is only nonzero when we are computing sensitivity to $k_{ll}$.

Substituting Eq. (17) into Eq. (13) allows the partial derivative of the heat flux, with respect to parameter $p_i$, to be arranged as

$$p_i \frac{\partial \vec{q}}{\partial p_i} = -\tilde{\mathbf{k}}(T) \cdot \nabla T_{p_i} - \left( \frac{d\tilde{\mathbf{k}}(T)}{dT} \cdot \nabla T \right) T_{p_i} - \begin{Bmatrix} k_{ll,i} \theta_i^{k_{ll}}(T) \dfrac{\partial T}{\partial x_l} \hat{e}_l & p=k_{ll} \\ 0 & \text{otherwise} \end{Bmatrix}. \quad (18)$$

The scalar $T_{p_i}$ has been moved outside the product in the second term on the right side of Eq. (18). The first term on the right side of Eq. (18) is present even for constant conductivity; the second term only appears for temperature dependent properties.

The remaining partial derivatives of temperature-dependent parameters in Eq. (12) are written by inspection from Eq. (16)

$$p_i \frac{\partial C(T)}{\partial p_i} = \frac{dC(T)}{dT} T_{p_i} + \begin{Bmatrix} C_i \theta_i^C & p=C \\ 0 & \text{otherwise} \end{Bmatrix} \quad (19)$$

$$p_i \frac{\partial \dot{e}'''(T)}{\partial p_i} = \frac{d\dot{e}'''(T)}{dT} T_{p_i} + \begin{Bmatrix} \dot{e}_i''' \theta_i^{\dot{e}} & p=\dot{e}''' \\ 0 & \text{otherwise} \end{Bmatrix}. \quad (20)$$

Substituting the partial derivatives from Eq. (18) through Eq. (20) into Eq. (12), the integral sensitivity equation for nonlinear heat conduction for an arbitrary parameter $p_i$ can be arranged as follows:

$$\begin{aligned} &\iiint_{\mathcal{V}} C(T) \frac{\partial T_{p_i}}{\partial t} d\mathcal{V} - \iint_{\mathcal{A}} [\tilde{\mathbf{k}}(T) \cdot \nabla T_{p_i}] \cdot d\vec{\mathcal{A}} + \iiint_{\mathcal{V}} \left[ \frac{dC(T)}{dT} \frac{\partial T}{\partial t} \right] T_{p_i} d\mathcal{V} \\ &- \iint_{\mathcal{A}} \left[ \frac{d\tilde{\mathbf{k}}(T)}{dT} \cdot \nabla T \right] T_{p_i} \cdot d\vec{\mathcal{A}} - \iiint_{\mathcal{V}} \left( \frac{d\dot{e}'''(T)}{dT} T_{p_i} \right) d\mathcal{V} \\ &= - \begin{Bmatrix} \displaystyle\iiint_{\mathcal{V}} C_i \theta_i^C(T) \frac{\partial T}{\partial t} d\mathcal{V} & p=C \\ 0 & \text{otherwise} \end{Bmatrix} + \begin{Bmatrix} \displaystyle\iint_{\mathcal{A}} \left[ k_{ll,i} \theta_i^{k_{ll}}(T) \frac{\partial T}{\partial x_l} \hat{e}_l \right] \cdot d\vec{\mathcal{A}} & p=k_{ll} \\ 0 & \text{otherwise} \end{Bmatrix} \\ &+ \begin{Bmatrix} \left( \displaystyle\iiint_{\mathcal{V}} \dot{e}_i''' \theta_i^{\dot{e}}(T) d\mathcal{V} \right) & p=\dot{e}''' \\ 0 & \text{otherwise} \end{Bmatrix}. \end{aligned} \quad (21)$$

Terms on the left side of Eq. (21) depend on the sensitivity coefficient and are present regardless of $p_i$. Right side contributions do not depend on the sensitivity coefficient ($T_{p_i}$) and are nonzero when $p_i$ is certain parameters—i.e., those appearing in the energy equation.

Boundary conditions for the sensitivity equation are obtained by performing the same differentiation procedure on the boundary conditions in Eq. (7) through Eq. (9). Prescribed flux boundary conditions for sensitivity are

$$p_i \frac{\partial}{\partial p_i}\int\int_{\mathcal{A}_b} \vec{q}\cdot d\vec{\mathcal{A}} = \int\int_{A_b} -\left[\tilde{\mathbf{k}}(T)\cdot\nabla T_{p_i} + \left(\frac{d\tilde{\mathbf{k}}(T)}{dT}\cdot\nabla T\right)T_{p_i}\right]\Bigg|_{\vec{x}_b}\cdot d\vec{A} + \int\int_{\mathcal{A}_b} p_i \frac{\partial \dot{q}_b''}{\partial p_i}\hat{n}\cdot d\vec{\mathcal{A}}, \tag{22}$$

where

$$p_i\frac{\partial \dot{q}_b''}{\partial p_i} = \begin{Bmatrix} \dot{q}_0'' & p=\dot{q}_0'' \\ 0 & \text{otherwise}\end{Bmatrix} \text{along } \vec{x}_{b_1} \tag{23a}$$

$$p_i\frac{\partial \dot{q}_b''}{\partial p_i} = p_i\frac{\partial \dot{q}_c''}{\partial p_i} = h(T)T_{p_i} + \frac{dh(T)}{dT}(T-T_\infty)T_{p_i} + \begin{Bmatrix} h_i\theta_i^h(T)(T-T_\infty) & p=h \\ 0 & \text{otherwise}\end{Bmatrix} \text{along } \vec{x}_{b_2} \tag{23b}$$

$$p_i\frac{\partial \dot{q}_b''}{\partial p_i} = p_i\frac{\partial \dot{q}_r''}{\partial p_i} = 4\varepsilon(T)\sigma T^3 T_{p_i} + \frac{d\varepsilon(T)}{dT}\sigma(T^4-T_r^4)T_{p_i} + \begin{Bmatrix} \varepsilon_i\theta_i^\varepsilon(T)\sigma(T^4-T_r^4) & p=\varepsilon \\ 0 & \text{otherwise}\end{Bmatrix} \text{along } \vec{x}_{b_3} \tag{23c}$$

The sensitivity boundary condition for a prescribed boundary temperature is

$$T_{p_i}(\vec{x}_{b_4}) = \begin{Bmatrix} T_b & p=T_b \\ 0 & \text{otherwise}\end{Bmatrix}. \tag{24}$$

The sensitivity initial condition is

$$T_{p_i}\big|_{t=0} = \begin{Bmatrix} T_0 & p=T_0 \\ 0 & \text{otherwise}\end{Bmatrix}. \tag{25}$$

*Discussion.* Sensitivity to an arbitrary parameter $p_i$ for nonlinear heat conduction is described by Eq. (21) through Eq. (25). Parameter $p_i$ can represent any parameter in the model. All parameters that can depend on temperature have been included. Table 1 summarizes the form of the right side of the sensitivity equation, boundary conditions, and initial condition for the possible parameters that $p_i$ represents. The left side of the equation is as given in Eq. (21), where RHS refers to the right side of this equation. This table parallels Table 4 presented in ([16]) for constant thermal properties.

The approach taken in this paper differentiates the describing equations to derive the sensitivity equation. Previous investigators ([11–15]) have differentiated the discretized equations. Although the two approaches should give the same numerical sensitivity, we believe there is additional insight available from the equation in this paper. The equations can be studied like conservation equations to provide physical insight to the sensitivity. The sensitivity equations are discussed next.

The first two terms in the sensitivity equation, Eq. (21), are identical in form to the first two terms in the describing equation for temperature, which represent the capacitance and diffusion effects in Eq. (4); an analogous term for the volumetric source in the temperature equation is not seen in the sensitivity equation. The third through the fifth terms on the left side of Eq. (21) are the result of parameters being temperature-dependent. All three terms contain the derivative of a parameter with respect to temperature and the scaled sensitivity coefficient; these terms are zero if those parameters are constant. The fourth term is similar to the convection term as it involves a surface integral. However, ''velocity'' is equal to a heat flux like term calculated using the derivative of the conductivity $(d\tilde{\mathbf{k}}(T)/dT\cdot\nabla T)$. The third and fifth terms on the left side are volumetric source-like terms, but are multiplied by the sensitivity coefficient.

When the parameter of interest is in the describing equation there is a right side contribution for the sensitivity equation in Eq. (21). (At most, one of these terms is nonzero for a particular parameter $p_i$.) The right side terms are completely known, assuming the temperature has been previously calculated. The form of these terms is analogous to those terms appearing in the temperature equation that contain the same parameters. However, the temperature-dependent parameter is represented with a single term from the approximation in Eq. (1)—i.e., we take only the $i^{\text{th}}$ term from the summation in Eq. (1).

Flux boundary conditions for the sensitivity equations in Eq. (23*a*) through Eq. (23*c*) have additional terms as well, with the exception of a specified constant flux in Eq. (23*a*). A term that contains temperature, and the derivative of the parameter with respect to temperature, is added for prescribed convection and radiation conditions. Similarly, an additional term is added if the sensitivity parameter, $p_i$, appears in the boundary condition. The term looks like the applied (convective or radiative) flux, except only a single term from the approximation of the temperature dependent parameter is included.

An important result is that even though the describing equations for temperature are *nonlinear*, the resulting equations for sensitivity are *linear*. It appears to be the rule that nonlinear field equations produce linear sensitivity equations; the authors are not aware of any exception published in the literature. An explanation for this outcome is that the process of differentiation only operates on one piece of the nonlinear term in the field equation at a time. Hence, by definition we will only have linear multiples for the derivative (sensitivity) when we differentiate. For example, consider a term that is nonlinear in $T$

$$g(T)T^2\nabla T. \tag{26}$$

The corresponding terms for sensitivity of $T$ to parameter $k$ are

$$\frac{dg(T)}{dT}\frac{\partial T}{\partial k}T^2\nabla T + g(T)2T\frac{\partial T}{\partial k}\nabla T + g(T)T^2\nabla\left(\frac{\partial T}{\partial k}\right). \tag{27}$$

Each term in Eq. (27) has a linear dependence on the derivative, $\partial T/\partial k$, regardless of the form of $g(T)$. We note that Eq. (27) is nonlinear in terms of $T$, but since we tacitly assume we will solve the field equation first this nonlinearity does not complicate matters. Finally, there is a difference between a nonlinear differential equation, which contains nonlinear multiples of the dependent variable (solution nonlinearity), and a field variable (temperature) which is a nonlinear function of the parameter (parameter nonlinearity). Parametric nonlinearity exists when the unscaled sensitivity equation is a function of the parameter. Parametric nonlinearity can exist, and often does, even though the solution is linear; most sensitivities for constant properties demonstrate this outcome ([16]). Solution nonlinearity, on the other hand, insures parametric nonlinearity due to the inherent dependence of the unscaled sensitivity equations on the field variable (temperature), and hence the parameter.

Linear sensitivity equations may allow for computational savings compared to a finite difference approximation of the sensitivity coefficient, where two nonlinear solutions are required to numerically approximate a sensitivity coefficient. At most, solving sensitivity equations will require the same computational effort as a finite difference approximation. Only when the temperature is obtained with a linear solution will computational efforts be similar.

**Table 1 Definition of various right-hand side and initial/boundary condition terms for the sensitivity coefficient equations. RHS refers to the right-hand side of Eq. (21).**

| $T_{p_i}$ | $RHS$ | $p_i \frac{\partial \dot{q}_b''}{\partial p_i}\Big\vert_{\vec{x}_{b_1}}$ | $p_i \frac{\partial \dot{q}_b''}{\partial p_i}\Big\vert_{\vec{x}_{b_2}}$ | $p_i \frac{\partial \dot{q}_b''}{\partial p_i}\Big\vert_{\vec{x}_{b_3}}$ | $T_{p_i}\big\vert_{\vec{x}_4}$ |
|---|---|---|---|---|---|
| $T_{k_{ll,i}}$ | $\iint_{\mathcal{A}} k_{ll,i}\theta_i^{k_{ll}}(T)\frac{\partial T}{\partial x_l}\hat{e}_l \cdot d\vec{\mathcal{A}}$ | 0 | $\left[h(T)T_{k_{ll,i}} + \frac{dh(T)}{dT}(T-T_\infty)T_{k_{ll,i}}\right]\Big\vert_{\vec{x}_2}$ | $\left[4\varepsilon(T)\sigma T^3 T_{k_{ll,i}} + \frac{d\varepsilon(T)}{dT}\sigma(T^4-T_r^4)T_{k_{ll,i}}\right]\Big\vert_{\vec{x}_3}$ | 0 |
| $T_{k_i}$ | $\iint_{\mathcal{A}} (k_i\theta_i^k(T)\nabla T \cdot d\vec{\mathcal{A}})$ | 0 | $\left[h(T)T_{k_i} + \frac{dh(T)}{dT}(T-T_\infty)T_{k_i}\right]\Big\vert_{\vec{x}_2}$ | $\left[4\varepsilon(T)\sigma T^3 T_{k_i} + \frac{d\varepsilon(T)}{dT}\sigma(T^4-T_r^4)T_{k_i}\right]\Big\vert_{\vec{x}_3}$ | 0 |
| $T_{C_i}$ | $-\iiint C_i\theta_i^C(T)\frac{\partial T}{\partial t}d\mathcal{V}$ | 0 | $\left[h(T)T_{C_i} + \frac{dh(T)}{dT}(T-T_\infty)T_{C_i}\right]\Big\vert_{\vec{x}_2}$ | $\left[4\varepsilon(T)\sigma T^3 T_{C_i} + \frac{d\varepsilon(T)}{dT}\sigma(T^4-T_r^4)T_{C_i}\right]\Big\vert_{\vec{x}_3}$ | 0 |
| $T_{\dot{e}_i'''}$ | $\iiint_{\mathcal{V}} \dot{e}_i'''\theta_i^{\dot{e}}(T)d\mathcal{V}$ | 0 | $\left[h(T)T_{\dot{e}_i'''} + \frac{dh(T)}{dT}(T-T_\infty)T_{\dot{e}_i'''}\right]\Big\vert_{\vec{x}_2}$ | $\left[4\varepsilon(T)\sigma T^3 T_{\dot{e}_i'''} + \frac{d\varepsilon(T)}{dT}\sigma(T^4-T_r^4)T_{\dot{e}_i'''}\right]\Big\vert_{\vec{x}_3}$ | 0 |
| $T_{\dot{q}_o''}$ | 0 | $\dot{q}_o''$ | $\left[h(T)T_{\dot{q}_o''} + \frac{dh(T)}{dT}(T-T_\infty)T_{\dot{q}_o''}\right]\Big\vert_{\vec{x}_2}$ | $\left[4\varepsilon(T)\sigma T^3 T_{\dot{q}_o''} + \frac{d\varepsilon(T)}{dT}\sigma(T^4-T_r^4)T_{\dot{q}_o''}\right]\Big\vert_{\vec{x}_3}$ | 0 |
| $T_{h_i}$ | 0 | 0 | $h(T)T_{h_i} + \frac{dh(T)}{dT}(T-T_\infty)T_{h_i}\Big\vert_{\vec{x}_2} +$ $[h_i\theta_i^h(T)(T-T_\infty)]\Big\vert_{\vec{x}_2}$ | $\left[4\varepsilon(T)\sigma T^3 T_{h_i} + \frac{d\varepsilon(T)}{dT}\sigma(T^4-T_r^4)T_{h_i}\right]\Big\vert_{\vec{x}_3}$ | 0 |
| $T_{\varepsilon_i}$ | 0 | 0 | $\left[h(T)T_{\varepsilon_i} + \frac{dh(T)}{dT}(T-T_\infty)T_{\varepsilon_i}\right]\Big\vert_{\vec{x}_2}$ | $\left[4\varepsilon(T)\sigma T^3 T_{\varepsilon_i} + \frac{d\varepsilon(T)}{dT}\sigma(T^4-T_r^4)T_{\varepsilon_i}\right]\Big\vert_{\vec{x}_3}$ $[\varepsilon_i\theta_i^{\varepsilon}(T)\sigma(T^4-T_r^4)]\Big\vert_{\vec{x}_3}$ | 0 |
| $T_{T_\infty}$ | 0 | 0 | $\left[h(T)T_{T_\infty} + \frac{dh(T)}{dT}(T-T_\infty)T_{T_\infty}\right]\Big\vert_{\vec{x}_2}$ $-h(T)T_\infty$ | $\left[4\varepsilon(T)\sigma T^3 T_{T_\infty} + \frac{d\varepsilon(T)}{dT}\sigma(T^4-T_r^4)T_{T_\infty}\right]\Big\vert_{\vec{x}_3}$ | 0 |
| $T_{T_r}$ | 0 | 0 | $\left[h(T)T_{T_r} + \frac{dh(T)}{dT}(T-T_\infty)T_{T_r}\right]\Big\vert_{\vec{x}_2}$ | $\left[4\varepsilon(T)\sigma T^3 T_{T_r} + \frac{d\varepsilon(T)}{dT}\sigma(T^4-T_r^4)T_{T_r}\right]\Big\vert_{\vec{x}_3}$ $-4\varepsilon(T)\sigma T_r^4\Big\vert_{\vec{x}_3}$ | 0 |
| $T_{T_b}$ | 0 | 0 | $\left[h(T)T_{T_b} + \frac{dh(T)}{dT}(T-T_\infty)T_{T_b}\right]\Big\vert_{\vec{x}_2}$ | $\left[4\varepsilon(T)\sigma T^3 T_{T_b} + \frac{d\varepsilon(T)}{dT}\sigma(T^4-T_r^4)T_{T_b}\right]\Big\vert_{\vec{x}_3}$ | $T_b$ |
| $T_{T_o}$ | 0 | 0 | $\left[h(T)T_{T_o} + \frac{dh(T)}{dT}(T-T_\infty)T_{T_o}\right]\Big\vert_{\vec{x}_2}$ | $\left[4\varepsilon(T)\sigma T^3 T_{T_o} + \frac{d\varepsilon(T)}{dT}\sigma(T^4-T_r^4)T_{T_o}\right]\Big\vert_{\vec{x}_3}$ | $T_o$ |

Sensitivity equations for *nonlinear* heat conduction have several additional left side terms compared to the temperature equation. In contrast, sensitivity equations for linear problems do not contain additional left side terms compared to the temperature equation. Sensitivity equations for the linear case are identical to the temperature equations, except for known right side contributions ([16]). This outcome for the linear case allows for potential computational savings by storing the global matrices after they are assembled for the temperature. Subsequent sensitivity problems can use the stored global matrices, and only a right side contribution needs to be calculated. If one can afford the storage for an LU decomposition algorithm, the decomposition can be used for efficiently solving for multiple sensitivities that only vary by their right-hand sides.

Emergy and Fadale [13] suggest solving the (linear) sensitivity equations for nonlinear heat conduction in an iterative procedure to avoid altering the structure of their finite element code. Global matrices are formulated and stored to calculate temperature. Subsequent sensitivity calculations use the same global matrices. The additional left side terms in the sensitivity equations, compared to the temperature equations are moved to the right side, and the equations are solved iteratively. This procedure saves recomputing the global matrices, but requires an iterative solution. Efficiency may be improved by adding the contributions from the additional terms to the stored global matrices that arise in the sensitivity equations. Then sensitivity can be solved in a linear manner. We do not reuse any of the assembled global matrices since we want to address very large problems for which storage of the global matrix is not practical.

**Numerical Solution.** The details of the numerical methods to solve the temperature and sensitivity equations are described in ([18]). An unstructured grid numerical solver based on a control volume finite element formulation for spatial discretization and implicit time discretization is used. The code architecture has been designed such that multiple equations can be solved. With this design, solving sensitivity equations requires writing additional element assembly routines for the desired sensitivity equations.

## Numerical Examples

**Verification Problem.** A one-dimensional slab of thickness, $L$, with temperature-dependent thermal conductivity is studied. The boundaries are isothermal. A mathematical description of the problem can be written as

$$\frac{d}{dx}\left(k(T)\frac{dT}{dx}\right)=0 \tag{28}$$

$$T|_{x=0}=T_L \tag{29a}$$

$$T|_{x=L}=T_R. \tag{29b}$$

Thermal conductivity is represented with two piecewise-linear segments

$$k(T)=\left\{\begin{array}{ll} k_1\left(1-\dfrac{T-T_1}{T_2-T_1}\right)+k_2\left(\dfrac{T-T_1}{T_2-T_1}\right), & (T_1\leqslant T\leqslant T_2) \\ k_2\left(1-\dfrac{T-T_2}{T_3-T_2}\right)+k_3\left(\dfrac{T-T_2}{T_3-T_2}\right), & (T_2< T\leqslant T_3) \end{array}\right\}. \tag{30}$$

An analytical solution can be obtained by integrating Eq. (28). Performing the integration over the two temperature segments that conductivity is defined and applying continuity between the two segments, gives quadratic equations to calculate temperature

$$\left\{\begin{array}{ll} \dfrac{\beta_1}{2}T^2+(k_1-\beta_1T_1)T+C_1 & (T_1\leqslant T\leqslant T_2) \\ \dfrac{\beta_2}{2}T^2+(k_2-\beta_2T_2)T+C_2 & (T_2< T\leqslant T_3) \end{array}\right\}=0. \tag{31}$$

In Eq. (31) the slopes of the linear conductivity segments are

$$\beta_i=\left(\frac{k_{i+1}-k_i}{T_{i+1}-T_i}\right),\quad i=1,2 \tag{32}$$

and the constant terms (with regard to the unknown temperature) are

$$\begin{aligned} C_1=&-\left[\frac{\beta_1}{2}T_L^2+(k_1-\beta_1T_1)T_L\right]\left(1-\frac{x}{L}\right) \\ &+\left\{\frac{(\beta_2-\beta_1)}{2}T_2^2+[(k_2-\beta_2T_2)-(k_1-\beta_1T_1)]T_2\right\}\frac{x}{L} \\ &-\left[\frac{\beta_2}{2}T_R^2+(k_2-\beta_2T_2)T_R\right]\frac{x}{L} \end{aligned} \tag{33}$$

$$\begin{aligned} C_2=&-\left[\frac{\beta_1}{2}T_L^2+(k_1-\beta_1T_1)T_L\right]\left(1-\frac{x}{L}\right) \\ &+\left\{\frac{(\beta_2-\beta_1)}{2}T_2^2+[(k_2-\beta_2T_2)-(k_1-\beta_1T_1)]T_2\right\}\left(\frac{x}{L}-1\right) \\ &-\left[\frac{\beta_2}{2}T_R^2+(k_2-\beta_2T_2)T_R\right]\frac{x}{L}. \end{aligned} \tag{34}$$

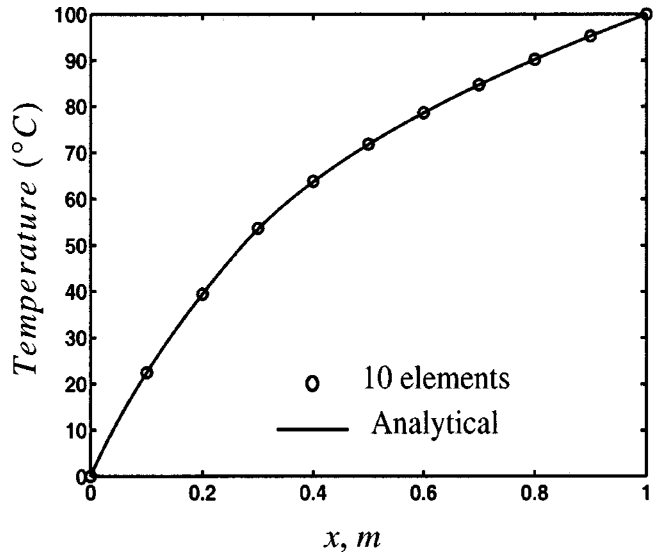


**Fig. 1 Temperature of a one-dimensional body with isothermal boundaries and temperature-dependent thermal conductivity represented with two piecewise linear segments**

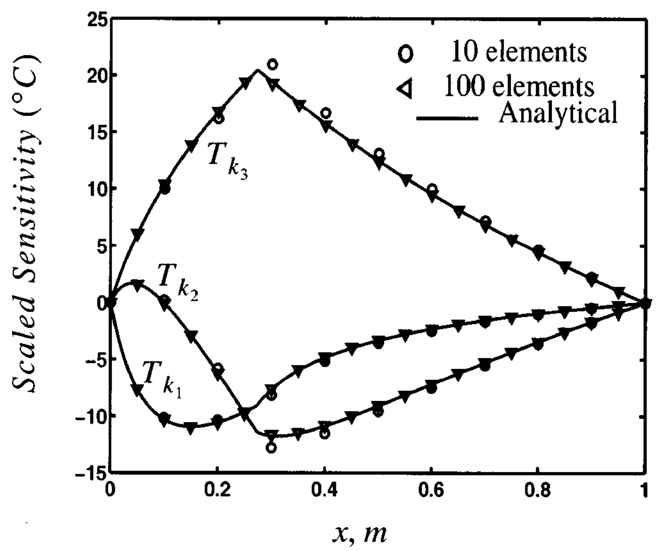


**Fig. 2 Sensitivity coefficients for parameters describing two piecewise linear segments representing temperature-dependent thermal conductivity for a one-dimensional body with isothermal boundaries**

To obtain temperature from Eq. (31), the physically meaningful root of the quadratic equations is taken. Analytical expressions for the sensitivity to $k_1$, $k_2$, and $k_3$ can be obtained by differentiating Eq. (31) with respect to these parameters.

Temperature is computed for a region of unit length ($L=1$ m). Boundary temperatures are maintained at $T_L=0\ °C$ and $T_R=100\ °C$. Conductivity is represented with two piecewise linear segments interpolating between conductivity values at three temperature: $k_1=1.0\ W/m\ °C$ at $T_1=0\ °C$, $k_2=2.0\ W/m\ °C$ at $T_2=50\ °C$, and $k_3=6.0\ W/m\ °C$ at $T_3=100\ °C$. The variation in this example represents a 4-to-1 change in the slope of the two piecewise linear segments representing $k(T)$. Figure 1 compares the numerically computed temperature with the analytical solution. Note that the temperature profile would be a straight line between the boundary temperatures for constant thermal conductivity. Agreement within 1.2 percent of the maximum temperature

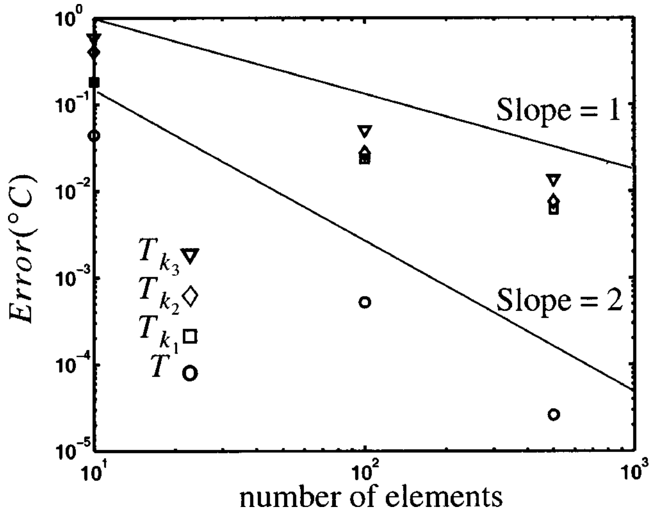


**Fig. 3 Grid convergence study at $x$=0.2 m for verification problem with temperature-dependent thermal conductivity**

is demonstrated with only 10 uniformly spaced elements. A comparison for sensitivity to the three components of thermal conductivity is shown in Fig. 2. Near the location where the piecewise linear segments join ($T(x\approx 0.27\ m)=50\ °C$), all three sensitivity coefficients have a sudden change in shape; the slope (derivative) of sensitivities to $k_2$ and $k_3$ changes sign at this location. With only ten elements the numerical and analytical results have the largest deviation near this region ($x\approx 0.27\ m$); the error is 4 to 8 percent of the maximum sensitivity value. This outcome demonstrates that a grid that results in small error for the temperature is not necessarily adequate for the sensitivity coefficients. It is expected that the largest errors are near the location joining the linear segments. Terms in the sensitivity equations in Eq. (21) to Eq. (25) contain the derivative of the conductivity with respect to temperature. For a piecewise linear representation, this derivative is discontinuous. Further refining the mesh to 100 uniformly spaced elements produces agreement within 1 percent of the analytical results for all sensitivity coefficients; see Fig. 2. Notice that the sensitivity to conductivity is zero on boundaries where temperature is specified.

A grid convergence study for the verification problem is shown in Fig. 3. Error is defined as the absolute difference between the numerical and analytical solutions. Results at location $x=0.2\ m$ are shown in the figure. Temperature demonstrates a second-order accuracy—that is, the error decreases with a slope of two as the spatial discretization is refined. Sensitivity, however, appears first-order accurate. Grid convergence at other spatial locations demonstrates the same order. For constant thermal properties the discretization schemes used to solve the temperature and sensitivity equations have been verified as second-order accurate ([16]). A possible explanation for the sensitivity solutions only achieving first-order accuracy could be the discontinuity in the derivative of piecewise-linear conductivity. This point is being studied further.

**Experimental Design.** An experimental configuration proposed to estimate thermal properties of a polyurethane foam is shown schematically in Fig. 4. Two nominally identical foam specimens are sandwiched about an electric heater. On the foam surface opposite the heater is an aluminum block. All components have cross-sectional dimensions of $w\times d$, whereas the thicknesses are $L_h$ for the heater, $L_f$ for the foam, and $L_a$ for the aluminum. The symmetry of the configuration permits quantifying the input flux by measuring the electrical power to the heater. By knowing the input flux and measuring temperatures elsewhere in the configuration, thermal properties of the foam can be estimated. In most cases a known input heat flux permits conductivity and volumetric heat capacity to be simultaneously estimated from a single experiment. The aluminum block maintains a nearly constant temperature on the backside of the foam. In the calculations that follow we assume the proposed apparatus can be modeled as symmetric one dimensional heat flow with a known applied heat flux $\dot{q}_0''$. The apparatus must be carefully designed to satisfy this assumption, but details associated with this design process are not considered further in this paper.

Optimal experimental conditions to estimate constant thermal properties for similar configurations are well known ([3–4]). The thickness of the foam and duration of the experiment should be selected such that the foam responds like a finite body heated by a constant flux on one surface and isothermal on the other surface. These conditions can readily be achieved in the laboratory for low conductivity materials. Based on *D*-optimally ([3]) the finite case is superior to the case where the foam responds thermally as a semi-infinite body. (These conclusions were reached while neglecting thermal effects of the heater and aluminum block.)

Optimum conditions to estimate temperature-dependent properties are less clear. A sequential method can be used to combine experiments at different temperature ranges ([1,19]). There are other approaches for estimating temperature dependent properties as well ([1]). In this paper the situation of estimating linearly varying temperature-dependent properties from a single experi-

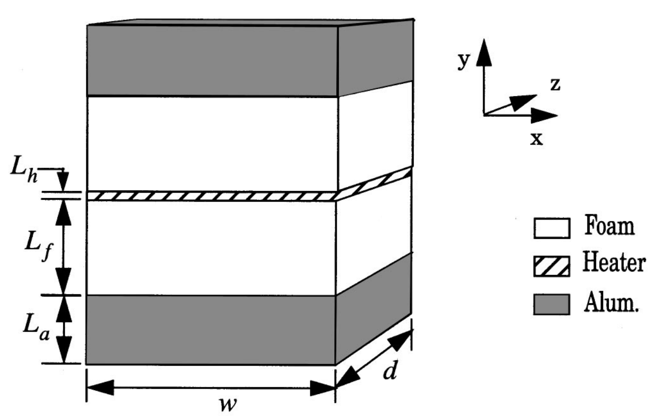


**Fig. 4 Experiment to estimate thermal properties of polyurethane foam**

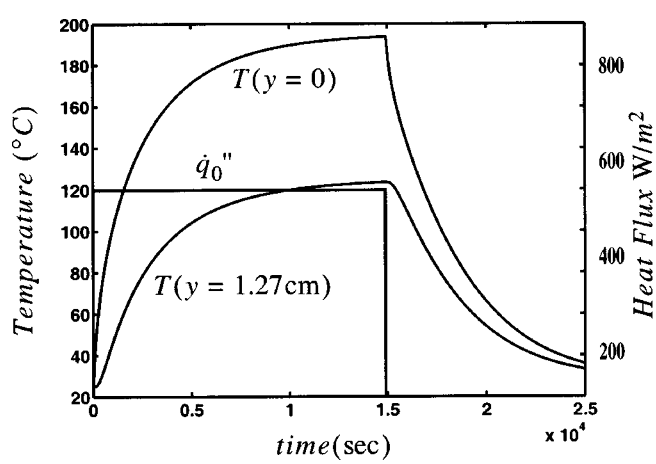


**Fig. 5 Temperature response for a foam thickness of 2.54 cm and linearly varying temperature-dependent properties (finite case)**

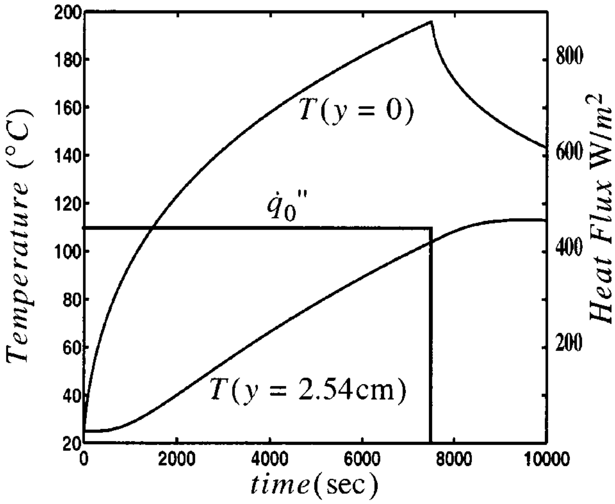


**Fig. 6 Temperature response for a foam thickness of 34.3 cm and linearly varying temperature-dependent properties (semi-infinite case)**

ment is addressed. Experimental design to estimate temperature-dependent properties is not, to our knowledge, available in the literature.

The case where properties (conductivity and volumetric heat capacity) vary linearly with temperature is considered. Foam thicknesses of 2.54 cm and 34.3 cm are used to compare experiments where the foam responds thermally as a finite and semi-infinite body, respectively. Although the foam specimens are obviously finite in size, if the thickness is large enough, thermal effects do not extend across its thickness. This case is referred to as semi-infinite. For low conductivity materials, like foam, the thermal response can be modeled as semi-infinite for appropriate time and length scales.

Temperature variable thermal properties for a foam density of 374 kg/m$^3$ are taken from ([20]); $k_f = 0.05$ $W/m$ $°C$ and $C_f = 0.433E + 0.6$ $J/m^3$ $°C$ at 25 °C and $k_f = 0.102$ $W/m$ $°C$ and $C_f = 1.19E + 06$ $J/m^3$ $°C$ at 200 $°C$. A thermal model of the heater assumes a thickness of 0.63 mm and constant properties of $k_h = 0.1$ $W/m$ $°C$ and $C_h = 2.3E + 06$ $J/m^3$ $°C$. These properties are equivalent to the effective properties estimated for a mica heater including contact resistance ([21]). Thermal properties of the aluminum are temperature-dependent, 2024 aluminum ([22]); the aluminum is not included in the model for the semi-infinite case. Simulated temperature responses assuming one dimensional symmetric heat flow in the configuration of Fig. 4 for a foam thickness of 2.54 cm (finite case) and 34.3 (semi-infinite case) are shown in Fig. 5 and Fig. 6, respectively. Two measurement locations are simulated for both cases: one at the heated surface ($y=0$) and the second within the foam. The finite case has the second location at the midplane of the foam thickness ($y=1.27$ cm). The semi-infinite case selects a second location 2.54 cm below the heated surface ($y=2.54$ cm). The applied heat flux is plotted with the temperature responses in Fig. 5 and Fig. 6.

The sensitivity coefficients for four parameters representing temperature-dependent properties in a finite body ($L_f = 2.54$ cm) are shown in Fig. 7. Sensitivities are shown at the surface of the foam ($y=0$) in the top figure and at the midplane of the thickness ($y=1.27$ cm) in the bottom figure. Sensitivity coefficients are normalized by the maximum temperature rise. Results for a semi-infinite body ($L_f = 34.3$ cm) are shown in Fig. 8 for locations at the surface of the foam (top figure) and 2.54 cm below the surface (bottom figure). As will be discussed later, the heating conditions and experimental duration for each case are selected because they maximize the $D$-optimality criteria to estimate the four parameters.

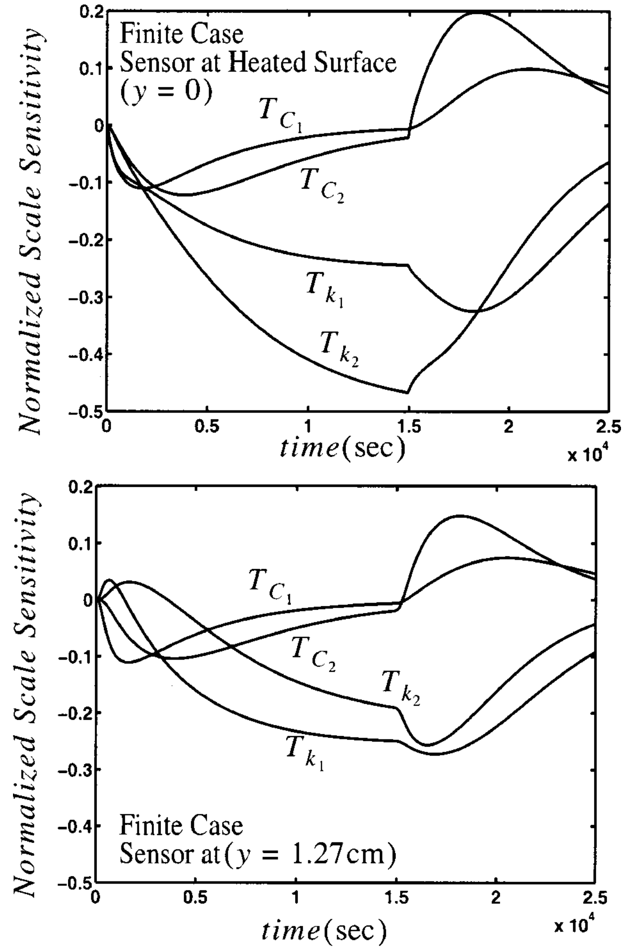


**Fig. 7 Sensitivity normalized by the maximum temperature rise for estimating linearly varying, temperature-dependent properties and a foam thickness of 2.54 cm (finite case)**

Sensitivity coefficients tend to be larger for the finite case in Fig. 7 than they are for the semi-infinite case in Fig. 8. The finite case has maximum values over 0.4, whereas the semi-infinite case has maximum less than 0.3. A second notable trend in the sensitivity plots is that the shapes for different parameters are more similar for the semi-infinite case than for the finite case, particularly for the sensor on the heated surface ($y=0$). Sensitivity for $k_2$ and $C_2$ and $k_1$ and $C_1$ have similar shapes in Fig. 8. (If thermal properties are constant, sensitivities for $k$ and $C$ have identical shapes at ($y=0$) and are perfectly correlated.) Finally, notice how dramatically the shape of the sensitivity coefficients change when the heat flux ends for the finite case. Sensitivity to $C_1$ and $C_2$ actually change sign after the heat flux ends. Such changes in the shape of the sensitivity coefficients improves the information available in an experiment. Sensitivity coefficients for the semi-infinite case have only a slight change in shape when the heating ends.

In the design of experiments to estimate thermal properties, we want the (scaled) sensitivity coefficients to be large and uncorrelated or have different shapes. However, drawing conclusions from sensitivity plots for multiple parameters and several locations can be difficult. It is further complicated in this case because different experimental conditions are compared. Normalizing the sensitivity coefficients by the maximum temperature rise provides some consistency; both experiments then have the same temperature range. Even with normalization it may be difficult to distinguish correlation between the sensitivity coefficients for different parameters. A criteria may be needed to gauge which experiment

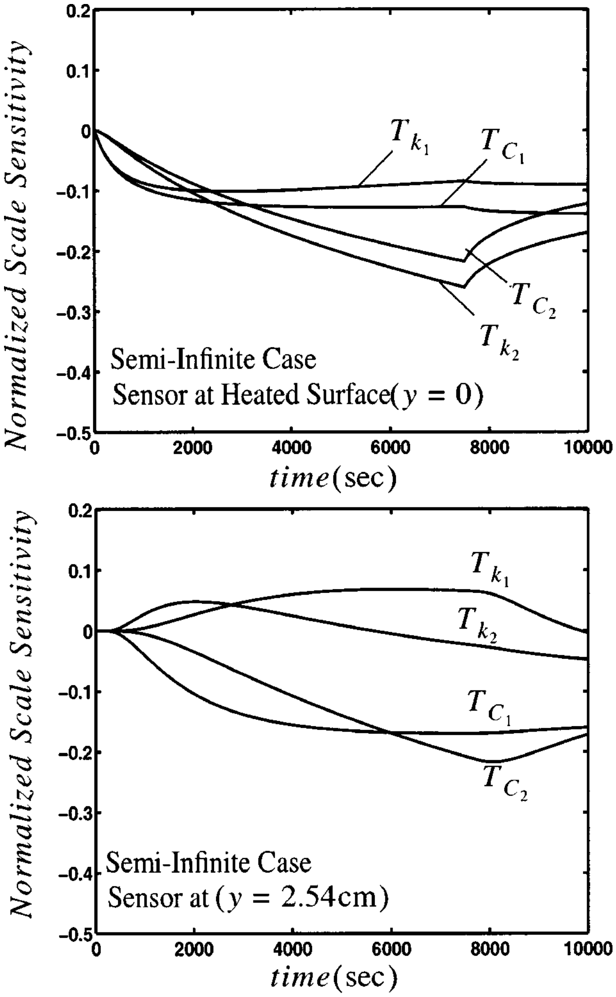


**Fig. 8 Sensitivity normalized by the maximum temperature rise for estimating linearly varying, temperature-dependent properties and a foam thickness of 34.3 cm (semi-infinite)**

is better. *D*-optimality ([3]) has been used to discriminate the optimal experiment. Emergy and Fadale [6] discuss several other criteria.

Sensitivity plots appear to indicate that the finite case is superior to the semi-infinite; sensitivities for the finite case are larger and have more varied shapes for the different parameters. To investigate which experiment is better, the *D*-optimality criteria is evaluated. The *D*-optimality criteria maximizes the determinant of the sensitivity matrix

$$\Delta \equiv |\mathbf{X}^T\mathbf{X}|. \tag{35a}$$

$\mathbf{X}$ is the sensitivity matrix;

$$\mathbf{X}^T = \left[\frac{\partial \mathbf{T}}{\partial p_1}, \frac{\partial \mathbf{T}}{\partial p_2}, \ldots, \frac{\partial \mathbf{T}}{\partial p_{N_p}}\right], \tag{36}$$

where $\mathbf{T}$ is a vector (length $N_sN_t$) of temperatures for each time and sensor location. Assuming there are $N_t$ discrete measurements in time, $N_s$ measurement locations, and $N_p$ parameters, the dimensions of $\mathbf{X}$ are $N_sN_t \times N_p$. The basis for this criteria is that it minimizes the volume of a confidence region. To provide a fair comparison for possibly different experimental conditions, constraints are introduced to the criteria. Measurements at the $N_s$ locations are assumed to be equally spaced in time at intervals $\Delta t$ up to time $t_f$. The maximum temperature rise of the experiment is $T_{max}$, and scaled sensitivity is used. To introduce these constraints, the optimality criteria is modified as

$$\Delta^+ \equiv \frac{|\mathbf{T}_{p_i}^T \mathbf{T}_{p_i}|}{(T_{max}^2 N_t N_s)^{N_p}}, \tag{37}$$

where $\mathbf{T}_{p_i}$ is the scaled sensitivity matrix.

The values of $\Delta^+$ are 4.0E-09 and 2.95E-10 for the finite and semi-infinite cases, respectively. The ratio is 13.6, meaning the volume of the confidence region is an order of magnitude smaller for the finite case. A finite body is superior for the experimental conditions and thermal properties selected. A range of the applied heat flux magnitude, heat flux duration, and experimental duration were investigated to identify the optimal experimental conditions for both cases. The sensitivity plots in Fig. 7 and Fig. 8 are for the conditions that gave the largest magnitude of $\Delta^+$. Superiority of the finite body case is consistent with the outcome for constant properties ([4]). However, for constant properties measurements at the heated surface alone are optimal.

## Conclusions

A general methodology to derive sensitivity equations for nonlinear heat conduction has been presented. Sensitivity equations were obtained by differentiating the continuum equations. These sensitivity equations were examined to provide insight to the factors that influence sensitivity coefficients. An important outcome was that the sensitivity equations are linear, even for the nonlinear temperature problems.

A verification problem demonstrated that while the numerical temperature was spatial second-order accurate, sensitivity calculations for temperature-dependent properties were only first-order accurate. Previous calculations for constant thermal properties have shown that the sensitivity calculations were second-order accurate. Sensitivity analysis was applied to design an experiment for estimating thermal properties varying linearly with temperature. Using the criteria *D*-optimality a finite geometry was demonstrated to be better than semi-infinite for estimating temperature-dependent properties.

## Acknowledgments

The authors would like to acknowledge comments concerning this work from Robert Cochran, Dean Dobranich, Shawn Burns, and Steve Kempka of Sandia National Laboratories. Sandia is a multiprogram laboratory operated by Sandia Corporation, a Lockheed Martin Company, for the United States Department of Energy under Contract DE-AC04-94AL85000.

## Nomenclature

$\mathcal{A}$ = area, $m^2$
$C$ = volumetric heat capacity, $J/m^3\text{-}°C$
$\dot{e}'''$ = energy source, $W/m^3$
$g$ = general temperature-dependent parameter
$h$ = convective heat transfer coefficient, $W/m^2\text{-}°C$
$k$ = thermal conductivity, $W/m\text{-}°C$
$k_{ll}$ = diagonal component of thermal conductivity tensor, $W/m°C$
$\tilde{\mathbf{k}}$ = thermal conductivity tensor, $W/m\text{-}°C$
$L$ = thickness, $m$
$N_g$ = number of parameters describing temperature dependence, $g$
$N_s$ = number of sensor locations
$N_t$ = number of discrete time measurements
$N_p$ = number of parameters
$p$ = arbitrary parameter
$\dot{q}''$ = heat flux, $W/m^2$
$\dot{q}_c''$ = convective heat flux, $W/m^2$
$\dot{q}_0''$ = constant value of heat flux, $W/m^2$
$\dot{q}_r''$ = radiative heat flux, $W/m^2$
$T, \mathbf{T}$ = temperature, temperature vector, $°C$

$T_b$ = boundary temperature, °C
$T_0$ = initial temperature, °C
$T_{p_i}$ = scaled temperature sensitivity coefficient for parameter $p_i$, °C
$T_r$ = radiation temperature, °C
$T_\infty$ = convection temperature, °C
$\mathbf{X}$ = sensitivity matrix
$\vec{x}_{b_1}$ = boundary with constant heat flux, $m$
$\vec{x}_{b_2}$ = boundary with convective heat flux, $m$
$\vec{x}_{b_3}$ = boundary with radiative heat flux, $m$
$\vec{x}_{b_4}$ = boundary with isothermal temperature, $m$
$\mathcal{V}$ = volume, $m^3$

**Greek**

$\beta$ = conductivity ratio, Eq. (32)
$\Delta, \Delta^+$ = optimality criteria
$\theta_j^g(T)$ = basis function for component $j$ of parameter $g$
$\phi_j^g(T)$ = derivative of basis function for component $j$ of parameter $g$
$\sigma$ = Stefan-Boltzmann constant.

## References


[1] Dowding, K. J., Beck, J. V., and Blackwell, B. F., 1999, ''Estimating Temperature-Dependent Thermal Properties of Carbon-Carbon Composite,'' J. Thermophys. Heat Transfer, **13**, No. 3, pp. 328–336.
[2] Dowding, K. J., Blackwell, B. F., and Cochran, R. J., 1999, ''Application of Sensitivity Coefficients for Heat Conduction Problems,'' Numer. Heat Transfer, Part B, **36**, No. 1, pp. 33–55.
[3] Beck, J. V., and Arnold, K., 1977, *Parameter Estimation in Engineering and Science* Wiley, New York.
[4] Taktak, R., Beck, J. V., and Scott, E., 1993, ''Optimal Experimental Design for Estimating Thermal Properties of Composite Materials,'' Int. J. Heat Mass Transf., **36**, No. 12, p. 2977.
[5] Taktak, R., 1992, ''Design and Validation of Optimal Experiments for Estimating Thermal Properties of Composite Materials,'' Ph.D thesis, Michigan State University, East Lansing, MI.
[6] Emery, A. F., and Fadale, T. D., 1996, ''Design of Experiments Using Uncertainty Information,'' ASME J. Heat Transfer, **118**, pp. 532–538.
[7] Fadale, T. D., Nenarokomov, A. V., and Emery, A. F., 1995, ''Two Approaches to Optimal Sensor Locations,'' ASME J. Heat Transfer, **117**, pp. 373–379.
[8] Coleman, H. W., and Stern, F., 1997, ''Uncertainties and CFD Code Validation,'' J. Fluids Eng., **119**, pp. 795–803.
[9] Coleman, H. W., and Steele, W. G., 1995, ''Engineering Applications of Experimental Uncertainty Analysis,'' AIAA J., **33**, No. 10, pp. 1888–1896.
[10] Fadale, T. D., and Emery, A. F., 1994, ''Transient Effects of Uncertainties on the Sensitivities of Temperatures and Heat Fluxes Using Stochastic Finite Elements,'' ASME J. Heat Transfer, **116**, pp. 808–814.
[11] Liu, W. K., Besterfield, G., and Belytschko, T., 1988, ''Transient Probabilistic Systems,'' Comput. Methods Appl. Mech. Eng., **67**, pp. 27–54.
[12] Liu, W. K., Belytschko, T., and Mani, A., 1986, ''Probabilistic Finite Elements for Nonlinear Structural Dynamics,'' Comput. Methods Appl. Mech. Eng., **56**, pp. 61–81.
[13] Emery, A. F., and Fadale, T. D., 1997, ''Handling Temperature Dependent Properties and Boundary Conditions in Stochastic Finite Element Analysis,'' Numer. Heat Transfer, Part A, **31**, pp. 37–51.
[14] Nicolai, B. M., and De Baerdemaeker, J., 1997, ''Finite Element Perturbation Analysis of Non-Linear Heat Conduction Problems with Random Field Parameters,'' Int. J. Numer. Methods Heat Fluid Flow, **7**, No. 5, pp. 525–544.
[15] Nicolai, B. M., and De Baerdemaeker, J., 1993, ''Computation of Heat Conduction in Materials with Random Variable Thermophysical Properties,'' Int. J. Numer. Methods Eng., **36**, pp. 523–536.
[16] Blackwell, B. F., Dowding, K. J., and Cochran, R. J., 1999, ''Development and Implementation of Sensitivity Coefficient Equations For Heat Conduction Problems,'' Numer. Heat Transfer, Part B, **36**, No. 1, pp. 15–32.
[17] Blackwell, B. F., and Dowding, K. J., 1999, ''Sensitivity Analysis and Uncertainty Propagation in a General Purpose Thermal Analysis Code,'' *Proceedings of the 3rd ASME/JSME Joint Fluids Engineering Conference*, July 18–23, 1999, San Francisco, CA.
[18] Blackwell, B. F., Cochran, R. J., and Dowding, K. J., 1998, ''Development and Implementation of Sensitivity Coefficient Equations for Heat Conduction Problems,'' *ASME Proceedings of the 7th AIAA/ASME Joint Thermophysics and Heat Transfer Conference*, ASME-HTD-Vol. **357-2**, pp. 303–316.
[19] Beck. J. V., and Osman, A. M, 1991, ''Sequential Estimation of Temperature-Dependent Thermal Properties,'' High Temperature-High Pressure **23**, pp. 255–266.
[20] Jin, G., Venkatesan, G., Chyu, M.-C., and Zheng, J.-X., 1998, ''Measurement of Thermal Conductivity and Heat Capacity of Foam Insulation During Transient Heating,'' AV-7569, Final Report, Department of Mechanical Engineering, Texas Tech. University, May 20, 1998.
[21] Dowding, K., Beck, J., Ulbrich, A., Blackwell, B., and Hayes, J., 1995, ''Estimation of Thermal Properties and Surface Heat Flux in a Carbon-Carbon Composite Material,'' J. Thermophys. Heat Transfer, **9**, No. 2, pp. 345–351.
[22] Incropera, F. P., and Dewitt, D. P., 1990, *Introduction to Heat Transfer*, 2nd Edition, Wiley, New York.